Chemical Science

EDGE ARTICLE

View Article Online
View Journal | View Issue

Cite this: *Chem. Sci.*, 2018, **9**, 70

A new generation of ferrociphenols leads to a great diversity of reactive metabolites, and exhibits remarkable antiproliferative properties†

Yong Wang,[ab] Patrick M. Dansette,[c] Pascal Pigeon,[ab] Siden Top,*[b] Michael J. McGlinchey,[d] Daniel Mansuy*[c] and Gérard Jaouen*[ab]

Organometallic compounds bearing the redox motif [ferrocenyl-*ene*-phenol] have very promising antiproliferative properties which have been further improved by incorporating pertinent substituents able to engender new mechanisms. Here we show that novel ferrociphenols bearing a hydroxypropyl chain exhibit strong antiproliferative effects, in most cases much better than those of cisplatin, tamoxifen, or of previously described ferrociphenols devoid of this terminal OH. This is illustrated, in the case of one of these compounds, by its IC_{50} values of 110 nM for MDA-MB-231 triple negative breast cancer cells and of 300 nM for cisplatin-resistant A2780cisR human ovarian cancer cells, and by its GI_{50} values lower than 100 nM towards a series of melanoma and renal cancer cell lines of the NCI-60 panel. Interestingly, oxidative metabolism of these hydroxypropyl-ferrociphenols yields two kinds of quinone methides (QMs) that readily react with various nucleophiles, such as glutathione, to give 1,6- and 1,8-adducts. Protonation of these quinone methides generates numerous reactive metabolites leading eventually to many rearrangement and cleavage products. This unprecedented and fully characterized metabolic profile involving a wide range of electrophilic metabolites that should react with cell macromolecules may be linked to the remarkable profile of antiproliferative activities of this new series. Indeed, the great diversity of unexpected reactive metabolites found upon oxidation will allow them to adapt to various situations present in the cancer cell. These data initiate a novel strategy for the rational design of anticancer molecules, thus opening the way to new organometallic potent anticancer drug candidates for the treatment of chemoresistant cancers.

Received 27th September 2017
Accepted 9th November 2017

DOI: 10.1039/c7sc04213b

rsc.li/chemical-science

Introduction

Despite recent advances in the treatment of certain cancers (for example, controlled targeting of the tumour, nanocapsule formulations, new biopharmaceutical agents with specific activity) the number of fatalities linked to cancers whose outcomes remain poor (*e.g.* melanoma, pancreatic and ovarian cancer, triple-negative breast cancer, glioma *etc.*), and which do not respond well to proapoptotic stimuli, continues to rise.[1–4] This has encouraged exploration of the potential role of inorganic compounds in this area, following the success of the coordination complexes of Pt, often in oxidation state +II, for which DNA is a primary but not the only target, and which are now in regular use.[5–8] Owing to a number of known issues with these complexes (relatively narrow therapeutic window, serious resistance and toxicity problems), recent research has turned towards organometallic complexes, principally those of gold and the Fe, Ru, Os triad, a novel approach that is now undergoing exponential growth.[9–19] These compounds often target the mitochondrial system or inhibit kinases or redox proteins overexpressed in cancer cells. Thus, they provide a new channel that offers a complementary solution to that of the platinum derivatives, bringing different targets and mechanisms of action into play.

Bioactive ferrocenes have provided a number of examples over the last few years to illustrate this approach, using a variety of synthetic strategies.[20–31] The ferrociphenols stand out from the crowd of current candidates owing to the advanced state of biological studies in the area, and also because of the rich variety of their mechanisms of action.[32–36] This richness is due to their ability to generate the redox motif {ferrocenyl-*ene*-phenol} in the cancer cell. The motif's activity can be modulated

[a]*PSL, Chimie ParisTech, 11 rue Pierre et Marie Curie, F-75005 Paris, France*
[b]*Sorbonne Universités, UPMC Univ Paris 6, UMR 8232 CNRS, IPCM, Place Jussieu, F-75005 Paris, France. E-mail: siden.top@upmc.fr; gerard.jaouen@upmc.fr*
[c]*Laboratoire de Chimie et Biochimie Pharmacologiques et Toxicologiques, UMR 8601 CNRS, Université Paris Descartes, PRES Paris Cité Sorbonne, 45 rue des Saints Pères, 75270 Paris Cedex 06, France. E-mail: Daniel.Mansuy@parisdescartes.fr*
[d]*UCD School of Chemistry and Chemical Biology, University College Dublin, Belfield, Dublin 4, Ireland*

† Electronic supplementary information (ESI) available: Experimental procedures for syntheses and biological evaluation, supplementary Fig. 1–8 and Tables 1–6, X-ray crystallographic data, cif file. CCDC 1527404. For ESI and crystallographic data in CIF or other electronic format see DOI: 10.1039/c7sc04213b

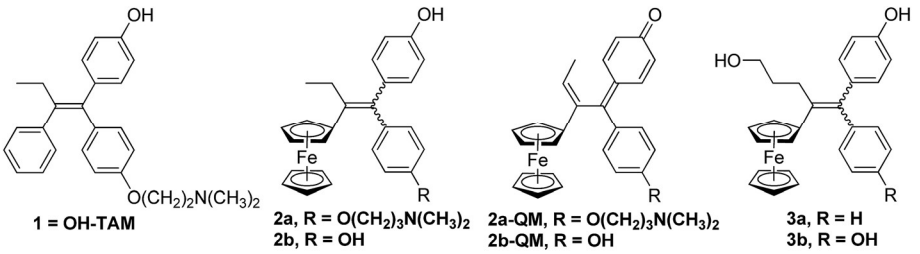

Fig. 1 Hydroxytamoxifen **1**, ferrociphenols **2** and their derived quinone methides **2-QM**, hydroxypropyl-ferrociphenols **3**.

by various substitutions, thus permitting a diversity of possible targets, an effect that is known to delay or prevent phenomena of drug resistance to a given biomolecule.

In particular we have been able to show that hydroxytamoxifen **1**, known for its antagonist effect on MCF-7 hormone-dependent (ERα+) breast cancer cells and for its lack of activity on hormone-independent (ERα−) MDA-MB-231 breast cancer cells, becomes strongly antiproliferative on both ERα+ and ERα− cells when modified to become the ferrociphenols **2a** (Fig. 1).[37] The IC_{50} of **2a** on MDA-MB-231 (ERα−) cells is 0.5 μM, and a cytostatic effect occurs *via* senescence.[38,39] This mechanism represents an alternative strategy to apoptosis in halting cell proliferation, and bypasses the problem of the resistance of cancers to proapoptotic stimuli. In addition, in those cancer cells for which apoptosis is possible, the apoptotic pathway is still operative. Moreover, compound **2a** interacts with a redox target overexpressed in certain cancers such as thioredoxine reductase.[40]

The basic chain in **2a** can be removed to give the ferrociphenol, **2b**, whose cytostatic effect on MDA-MB-231 cells is comparable to that of **2a**. Subsequently, we were able to show that quinone methides **2-QM**, arising from the initial oxidation of ferrocene Fe^{II} to the corresponding ferricinium Fe^{III} species, are active metabolites of compounds **2** (Fig. 1).[41–43] These compounds are active on cancer cells but not on healthy cells (astrocytes, melanocytes) where the redox effect is not observed.[44,45] The effectiveness of these two compounds, **2a** and **2b**, delivered by lipid nanocapsules (LNCs), has been studied on experimental subcutaneous models of triple-negative breast cancer and malignant glioma, respectively. In both cases, a significant slowing of tumor progression was observed, confirming the antiproliferative activity of these compounds.[46–48]

In our search for a new series of molecules surpassing the antiproliferative effect of the above products we have recently obtained promising results by introducing functional groups at the end of the alkyl chain.[49] In particular, the hydroxypropyl derivative **3b** (Fig. 1) exhibited exceptional antiproliferative activity against *inter alia* liver hepatocellular carcinoma cells (HepG2) and triple negative breast cancer cells (MDA-MB-231) with IC_{50} values of 0.07 and 0.11 μM, respectively.[49] Chemical oxidation of **3a**/**3b** yielded an unprecedented tetrahydrofuran-

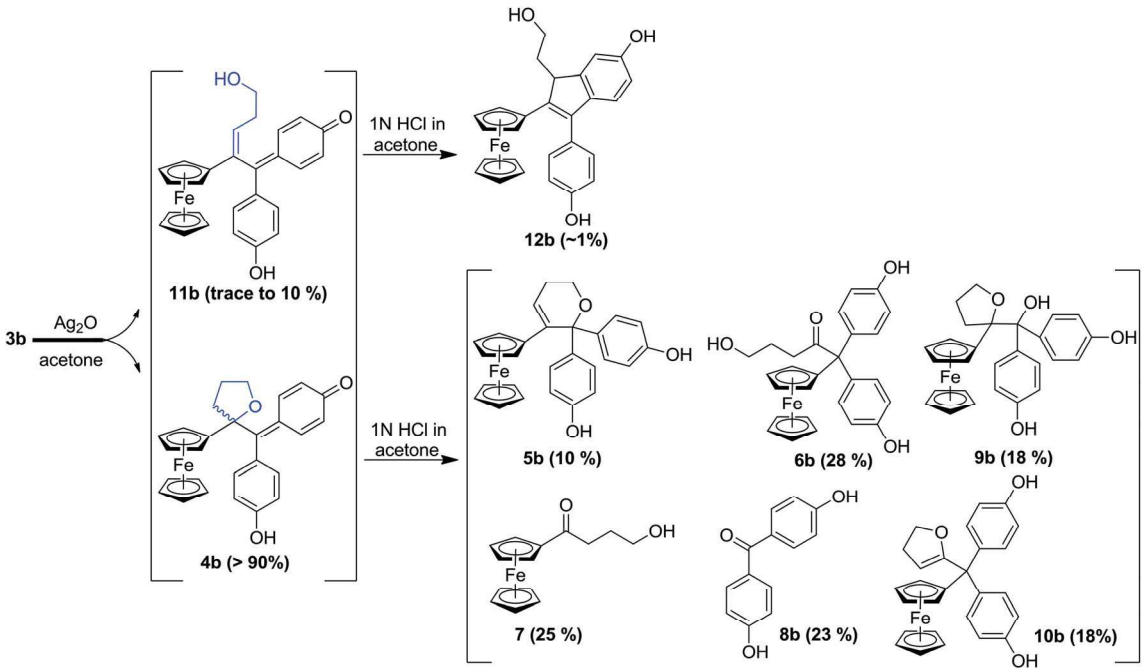

Fig. 2 Quinone methides **4b** and **11b** from the oxidation of hydroxypropyl-ferrociphenols **3b** and subsequent protonation (similar results were obtained in the case of **3a**). Yields are based on starting compound **3b**, but note that cleavage of the C–C bond of **9b** yields both **7** and **8**.

substituted quinone methide (QM), **4a**/**4b**, *via* an internal cyclization of the hydroxyl-alkyl chain (Fig. 2). The ferrocenyl group in **3** plays a key role not only as an intramolecular reversible redox "antenna" but also as a stabilized carbenium ion "modulator".[49] Moreover, the presence of the oxygen heterocycle in **4** enhances its stability and leads to a unique chemical evolution profile, leading to products **5**, **6**, **7**, and **8** (Fig. 2) that were characterized spectroscopically (NMR, HRMS) or by X-ray crystallography.[49]

To further explore the promising antiproliferative properties of compounds **3a** and **3b** and their unique evolution profile upon oxidation, we have studied the fate of these compounds upon chemical oxidation or after metabolism by liver microsomes, in the presence of nucleophiles such as thiols that are present in proteins and nucleic acids. The antiproliferative properties of compounds **3** and their metabolites towards breast cancer cells were evaluated. Moreover, we have compared the activities of **3b**, **2b** and cisplatin towards ovarian cancer cell lines sensitive or resistant to cisplatin. The antiproliferative effects of **3b** were also evaluated by the National Cancer Institute on the NCI-60 human tumor cell line panel.[50] The obtained data showed a quite remarkable profile of antiproliferative activities of **3b**, and the formation of a surprisingly great diversity of reactive metabolites upon metabolic oxidation of **3b**.

Results

Chemical oxidation of the hydroxypropyl-ferrociphenols, 3a and 3b

To compare the behaviour of the acyclic QMs, such as **2b-QM**, and the tetrahydrofuran-substituted QMs **4a** and **4b**, we have explored the effects of several oxidants (including Ag_2O, MnO_2, H_2O_2) on their precursors **3a** and **3b**. As shown in Fig. 2, generation of the QMs **4**, followed by addition of 1 N HCl aqueous solution in acetone, not only led to the previously reported molecules **5–8**, but also to two new products, **9**, the 1,6-adduct of water to **4**, and **10**, the product of ferrocenyl migration in a pinacol-type rearrangement (Fig. S1†). In contrast, protonation of **4b** with HCl in dry diethyl ether yielded only two major products, **5b** (35%) and **6b** (47%). Compounds **7** and **8** were major products only when the protonation was carried out in acetone, a well-known solvent for triplet state photosensitized processes.[51]

The novel products **10**, arising from the protonation of **4**, can come from a 1,2-migration of the ferrocenyl moiety, thus generating a cation stabilized by the adjacent oxygen in the five-membered ring (Fig. S1†). These rearrangement products, in which the 2,3-dihydrofuran ring and the ferrocenyl moiety are attached to the same carbon center, were unequivocally characterized spectroscopically, and by X-ray crystallography in the case of **10b** whose structure appears in Fig. 3.

In addition to the products described above, the hydroxy-alkenyl quinone methides **11** (Fig. 2), analogous to the vinylic **2-QM**, were also formed, and identified by HPLC and ^{1}H NMR, even though their existence was somewhat transient. Thus, in the case of **11b** for instance, the appearance of a multiplet and a triplet at 1.60 and 6.43 ppm, respectively, indicated the formation of a double bond within the starting hydroxypropyl group (Fig. S3†). The yield of **11b** (varying from trace to 10%, relative to **4b**, as monitored by ^{1}H NMR) was dependent on the concentration of its precursor **3b** (from 2 to 100 mM), and the quantity of oxidant (one to five equivalents of Ag_2O). Indene product **12b** resulting from an acid-catalyzed cyclisation of the hydroxy-alkenyl quinone methide **11b**, as previously found in the case of vinylic quinone methides, **2-QM**,[52] (Fig. S2†) was also formed in low amounts upon oxidation of **3b**. The identities of the new QM, **11b**, and its corresponding indene, **12b**, were also confirmed by their characteristic UV-VIS spectra (λ_{max} ~560 nm and ~320 nm for vinyl QMs and indene derivatives, respectively[53]).

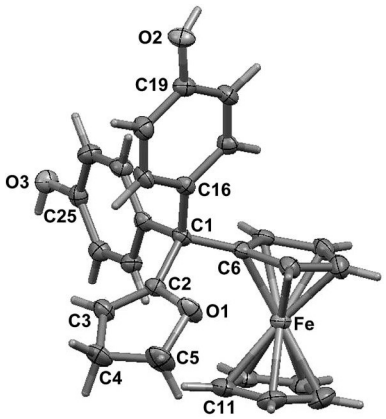

Fig. 3 Molecular structure of **10b** (thermal ellipsoids are shown at 50%).

In this case, we found for the first time that chemical oxidation of the hydroxypropyl-ferrociphenol, **3**, yields two kinds of quinone methides. Since the tetrahydrofuran-QMs **4**, and the hydroxyalkenyl-QMs **11**, arise from a common precursor, a ferrocenyl cation **13** (Fig. 4) initially generated by a two-electron oxidation of **3**, the observed **4**/**11** ratio is the result of a competition between intramolecular cyclization with subsequent deprotonation to form **4**, *versus* deprotonation to generate the conjugated carbon–carbon double bond in **11**. This ratio and the proportions of the observed products **5–12** were greatly dependent on the nature of the used oxidant and acid, and on the amounts of oxidant relative to **3**.

Reactions of the tetrahydrofuran-substituted QMs 4a and 4b toward nucleophiles

The reactions of this new type of electrophilic intermediate with various nucleophiles, including thiols such as mercaptoethanol (ME), *N*-acetyl-L-cysteine methyl ester (NACM) and glutathione (GSH), were studied. Compounds **3a** or **3b** were first treated with silver oxide to generate **4a** or **4b** at room temperature and, after removal of excess Ag_2O, the nucleophiles were added. In each case, progress of the reaction was monitored by TLC or HPLC.

Methanol reacted *via* 1,6-addition to yield the pinacol-type methyl ethers, **14**, in good yield (Fig. 4). By contrast, ME in acetone gave a poor yield of the 1,6-adducts, **15**. However, both the rate of reaction and the yield of **15** were greatly enhanced by

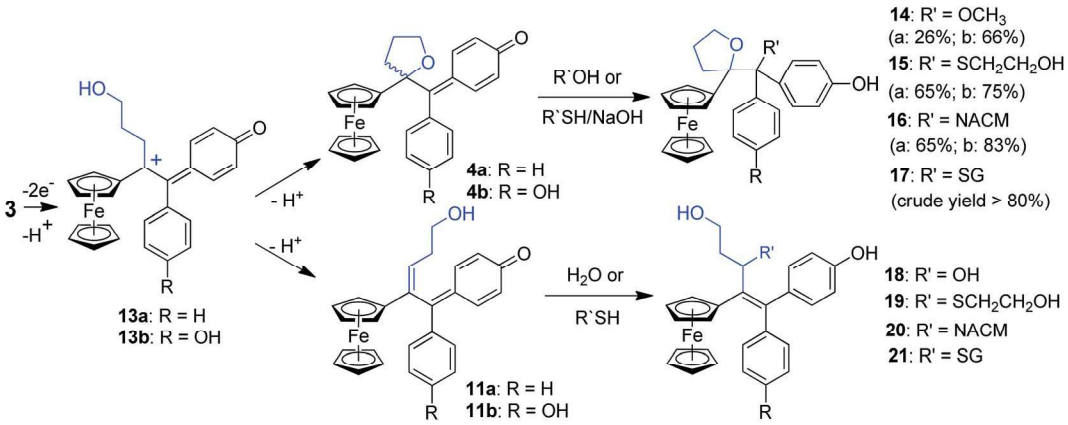

Fig. 4 1,6- and 1,8-adducts to quinone methides **4** and **11**.

addition of NaOH to form the thiolate. Analogous reactions with NACM and glutathione in the presence of NaOH led to the corresponding 1,6-adducts, **16** and **17**, respectively, in very good yields (Fig. 4). The adducts **14–16** were characterized by ^{1}H NMR spectroscopy and mass spectrometry. Complete purification of **17** was not possible because of the high polarity of the GS function, and a crude sample was obtained.

When treated under more physiological conditions (50 mM phosphate buffer, pH 7.4, 37 °C), **4b** led after 30 min to the aforementioned products **5b–10b** in low to moderate yields. Under these conditions, the half-life of 0.15 mM **4b** was approximately 25 min. However, incubation of **4b** under these conditions in the presence of ME, NACM or GSH gave the corresponding 1,6-adducts, **15b**, **16b** or **17b**, respectively, in yields greater than 80%. In the presence of these thiols, the half-life of **4b**, as monitored by UV-VIS spectroscopy, was markedly reduced to 1.5, 3.2 and 2.3 min, respectively. It is noteworthy that all these 1,6-adducts were progressively transformed into 4-hydroxy-1-ferrocenylbutan-1-one **7** and diarylmethanone **8** (Fig. S4–S8†). However, they were stable for at least a week in the absence of air and light.

Oxidation of compounds 3a and 3b by horseradish peroxidase (HRP)

Incubation of **3a** and **3b** with HRP and H_2O_2 for 30 min (0.25 mM **3**, 0.1% HRP and 4 equivalents of H_2O_2) led to products that have been observed upon chemical oxidation of **3a** and **3b** and that were found to derive from quinone methides **4** and **11**. The proportions of these products varied as a function of the used conditions (**3**/HRP/H_2O_2 ratios, reaction time) (Tables S2 and S3†). However, compounds **7** and **8** were always the major oxidation products, and the products deriving from the hydroxyalkenyl-QM **11** were only formed in trace amounts. When low amounts of HRP and H_2O_2 were used (0.1 mM **3**, 0.02% HRP and one equivalent of H_2O_2) their total yield increased to about 10%.

Oxidative metabolism of compounds 3a and 3b by liver microsomes

Incubation of **3a** or **3b** with rat liver microsomes in the presence of NADPH, the reducing agent necessary for the activity of microsomal monooxygenases, led to the formation of all the products that were observed upon oxidation of **3a** or **3b** by chemical oxidants or HRP and H_2O_2 (Tables S2 and S3†). They were characterized by comparison of their HPLC retention times, and also their MS and MS-MS characteristics, with those of authentic samples obtained by chemical synthesis. None of these metabolites were observed under identical incubations without NADPH. Incubations of **3a** and **3b** with human liver microsomes under identical conditions led to results very similar to those obtained with rat liver microsomes. Ketones **7** and **8** were always the major products and represented more than 40% of all metabolites, whereas dihydropyran **5** was formed in lower amounts and compounds **6**, **9** and **10** were formed in trace amounts. These data showed that microsomal oxidation of **3** mainly led to products deriving from QM **4**. However, minor formation of metabolites **12** and **18**, that derived from the hydroxyalkenyl quinone methide **11**, showed that both QM **4** and **11** were formed as initial oxidation products. It is noteworthy that a decrease of the microsomal proteins concentration in the incubate led to an increase of the ratio of **18** relative to all other metabolites (from less than 5% to about 10% when decreasing the protein concentration by a factor 1.7). This result is to be compared to analogous data obtained in oxidation of **3** with chemical oxidants or HRP and H_2O_2, and indicates that the intermediate formation of QM **4** is the major pathway occurring in oxidation of **3**, but that the relative importance of the formation of QM **11** is greater under milder oxidizing conditions (use of lower oxidant or oxidation catalyst amounts).

Incubation of ferrociphenols **3a** and **3b** with rat liver microsomes in the presence of NADPH and various thiols, led to QM-thiol adducts, as well as the metabolites we have already observed under identical conditions in the absence of thiols (Tables S2 and S3†). All the 1,6- and 1,8-thiol adducts (**15–17** and **19–21**, respectively, Fig. 4) arising from their corresponding QM precursors were detected in trace to moderate amounts, and were characterized by comparison of their HPLC retention times and MS spectra with those of authentic samples. The 1,6-adducts are less polar and exhibit longer retention times than their 1,8-adduct counterparts; moreover, their mass spectral

fragmentation patterns were also significantly different (Table S4†). In microsomal incubations of **3** in the presence of ME or NACM, ketones **7** and **8** were still the major products and represented more than 40% of all metabolites, whereas the proportions of 1,6-thiol adducts relative to all metabolites remained below 10% and only low amounts of 1,8-thiol adducts were observed under these conditions. Interestingly, incubation of **3** with liver microsomes, in the presence of NADPH and GSH, gave **17** as a major GSH adduct (40% of all metabolites) with a minor amount of the 1,8-GSH adduct **21**. Upon increasing the protein concentration, the relative proportion of **7** and **8** increased and **17** was still formed in an about 5–10% yield relative to all metabolites whereas **21** was only formed in trace amounts (Tables S2 and S3†). Accordingly, incubation of authentic 1,6-thiol adducts **15–17** with liver microsomes and NADPH mainly led to **7** and **8**. The stability of these 1,6-thiol adducts towards microsomal oxidation is as follows: **17** > **16** > **15**, suggesting that the size and polarity of the thiol substituents adjacent to the tetrahydrofuran ring play an important role in their microsomal oxidation into **7** and **8**.

Antiproliferative effects of 3a and 3b and their oxidation metabolites against TNBC MDA-MB-231 cells

The antiproliferative activities of compounds **3a** and **3b**, and of the products derived from their oxidation in the presence or absence of thiols, against hormone-refractory breast cancer MDA-MB-231 cells, are shown in Table 1. Compounds **3a** and **3b** were the most active, with IC_{50} values of 1.1 and 0.11 μM, respectively. However, the transient intermediates appearing during their oxidative metabolism, the quinone methides **4**, their water 1,6-adducts **9**, and their thiol 1,6-adducts, **15** and **16**, were also active with IC_{50} values between 2 and 10 μM; these data are in sharp contrast with the very low activity of the final major metabolites **7** and **8** that exhibited IC_{50} values above 100 μM. These IC_{50} values of intermediates **4**, **9**, **15** and **16** are quite remarkable, especially if one takes into account their instability in the assay medium, and possible problems of cell penetration. This suggests that they should have potent antiproliferative effects when they are formed inside the cell, close to important cell targets, upon oxidative metabolism of **3**.

Table 1 IC_{50} values for selected ferrocenyl compounds towards MDA-MB-231 cells

Compound	IC_{50}[a] (μM)	Compound	IC_{50}[a] (μM)
2b	0.64 ± 0.06	**5b**[b]	2.03 ± 0.79
3a[b]	1.16 ± 0.02	**6b**[b]	4.14 ± 1.33
4a (QM)[b]	1.89 ± 0.08	**7**[b]	≈150
6a	8.17 ± 1.56	**8b**[b]	≈295
9a (1,6-OH)	6.12 ± 0.97	**10b**	9.92 ± 0.78
15a (1,6-ME)	7.51 ± 0.52	**9b** (1,6-OH)	9.60 ± 1.29
16a (1,6-NACM)	4.36 ± 0.26	**14b** (1,6-OMe)	3.07 ± 0.01
3b[b]	0.11 ± 0.02	**15b** (1,6-ME)	2.36 ± 0.14
4b (QM)[b]	4.39 ± 1.47	**16b** (1,6-NACM)	2.43 ± 0.4

[a] Measured after 5 days of culture (mean of two independent experiments ± SD). [b] Values taken from ref. 49.

Cytotoxicity studies of compounds 2b and 3b against cisplatin-sensitive and cisplatin-resistant human ovarian cancer cell lines

The cytotoxic activities of the vinyl derivative, **2b**, and the hydroxypropyl complex, **3b**, were further evaluated against two human ovarian cancer cell lines, cisplatin-sensitive A2780 and cisplatin-resistant A2780cisR cells (Table 2). Their activities toward a healthy human lung fibroblast cell line, MRC-5, were also measured. The A2780cisR variant is known to encompass all of the known major mechanisms of resistance to cisplatin:[54] decreased drug transport, enhanced DNA repair/damage tolerance, elevated cellular thiol (GSH) level, and blockage of cell-death pathways. As shown in Table 2, **2b** and **3b** showed a potent antiproliferative activity not only against wildtype A2780, but also against resistant A2780cisR cells, with a resistance factor smaller than one, contrary to cisplatin (CDDP) that exhibits a resistance factor of about ten.[55] It is noteworthy that **3b** showed a 7-fold greater cytotoxicity than **2b** against A2780 and A2780cisR cells, and a 38-fold greater cytotoxicity than cisplatin against A2780cisR cells. These observations suggest that compound **3b** may be much less affected by high cellular GSH levels or other physiological adaptations occurring in resistant cancer cells. Moreover, **3b** is approximately sixteen times less toxic towards normal human cells MRC-5 than towards A2780 cancer cells, whereas **2b** and cisplatin have lower selectivity factors of approximately 2 and 8.5, respectively.

Antiproliferative effects of 2b and 3b on the NCI cell line panel

The antiproliferative effects of **3b** were further evaluated by the National Cancer Institute on the NCI-60 human tumor cell line panel,[50] which consists of approximately 60 cell lines within nine tumor type subpanels. They were compared to those found for compound **2b**,[56] tamoxifen (TAM) and cisplatin (CDDP) (Fig. 5, Tables S5 and S6†). The cells were treated for 48 h at five concentrations ranging from 0.01 to 100 μM. Three endpoints were calculated: GI_{50} (50% growth inhibition concentration), TGI (100% growth inhibition concentration), and LC_{50} (50% lethal concentration). Compounds **2b** and **3b** exhibited a broad spectrum of activity over a 3-log range of GI_{50}, which means that these compounds are not indiscriminately cytotoxic against cellular growth. Compounds **2b** and **3b** (mean GI_{50} around 0.5 μM and 0.4 μM respectively) are approximately ten-fold and

Table 2 IC_{50} values for compounds **2b**, **3b** and cisplatin (CDDP) towards human ovarian cancer cells and normal human fibroblast cells

	IC_{50}[a] (μM)				
Compound	A2780	A2780cisR	RF[b]	IC_{50}[a] (μM) MRC-5	SF[c]
2b	3.5 ± 0.94	2.3 ± 0.7	0.66	7.28 ± 0.39	2.1
3b	0.53 ± 0.01	0.30 ± 0.03	0.57	8.54 ± 0.32	16.1
CDDP[d]	1.2 ± 0.20	11.5 ± 0.3	9.6	16.2 ± 0.6	8.5

[a] Measured after 72 h of culture (mean of three independent experiments ± SD). [b] RF, resistance factor: IC_{50} toward A2780cisR/IC_{50} toward A2780 ratio. [c] SF, selectivity factor: IC_{50} toward MRC-5/IC_{50} for A2780 ratio. [d] Values taken from ref. 55.

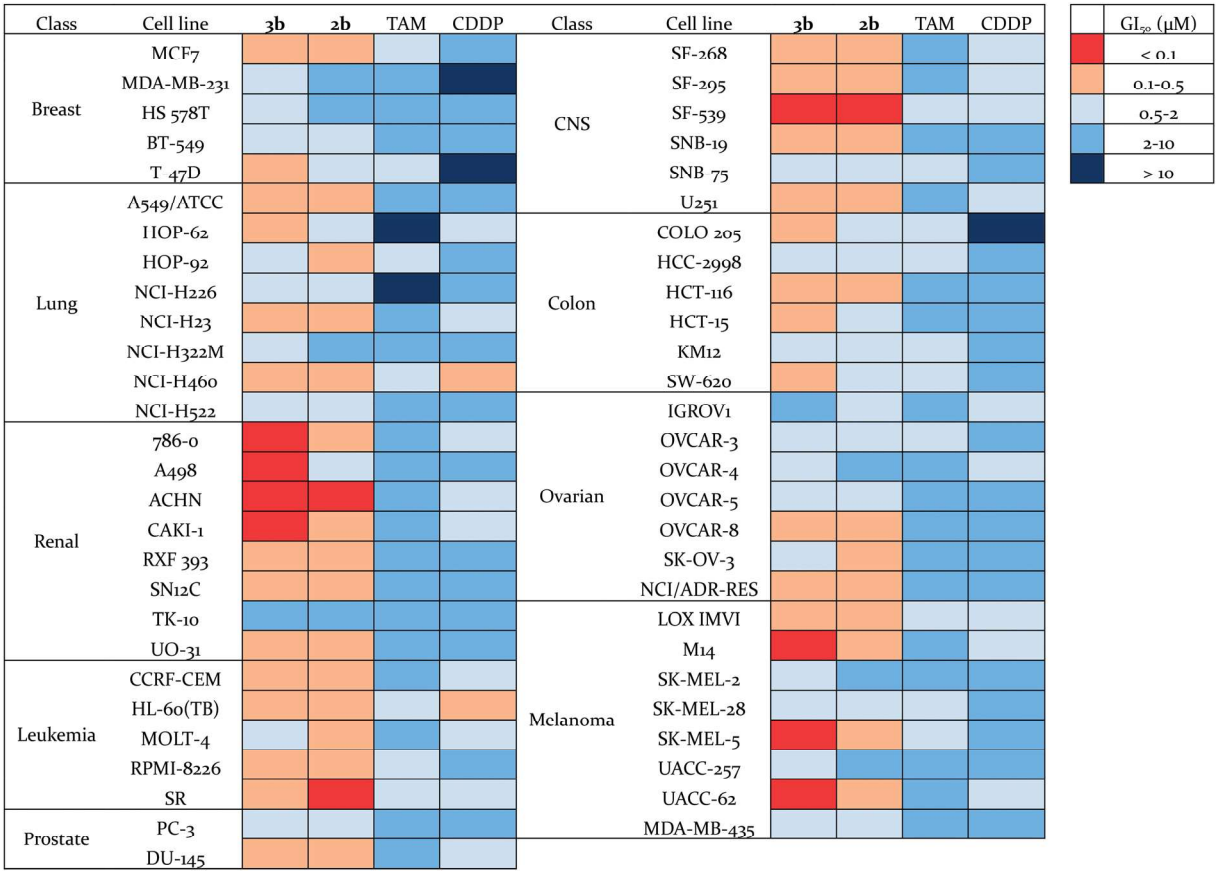

Fig. 5 Heat map for GI_{50} values of **3b**, **2b**, TAM and CDDP. The deep red color indicates the highest activity, whereas the deep blue color represents the lowest activity.

thirty-fold more potent (in terms of GI_{50} values) than tamoxifen and cisplatin, respectively (Table S6†). Compound **3b** shows a high potency towards a wide range of cancer cell lines, with a particularly high activity against renal, melanoma and CNS cancer cell lines. Thus, its GI_{50} values for M14, SK-MEL-5, UACC-62 (3/8 melanoma sub-lines) and 786-0, A498, ACHN, CAKI-1 (4/8 renal cancer sub-lines) were found to be lower than 100 nM. Renal cancers are often chemoresistant because of the high expression of multi-drug resistant (MDR1) protein, and elevated level of P-glycoprotein in renal cancer cells.[57,58] Melanoma is a highly aggressive neoplasm and has a poor response to conventional chemotherapy,[59] meaning that intrinsic drug resistance is also a serious problem in melanoma treatment. The high potency of compound **3b** towards the phenotypes of renal cancer and melanoma is promising for the use of such organometallic complexes for the treatment of such resistant cancers.

Discussion

The novel ferrociphenols **3** bearing a terminal OH group in their alkyl moiety exhibit strong antiproliferative properties, very frequently much better than those of ferrociphenols **2**, cisplatin or tamoxifen. This is illustrated, in the case of **3b**, by its IC_{50} values of 110 nM for MDA-MB-231 breast cancer cells (Table 1) and of 530 nM for A2780 human ovarian cancer cells (Table 2), and by its GI_{50} values lower than 100 nM towards a series of renal cancer and melanoma cells (Fig. 5). Interestingly, compound **3b** is quite active towards cisplatin-resistant A2780cisR ovarian cancer cells (Table 2).

Ferrociphenols **3** also exhibit a remarkable profile of metabolic oxidation, when compared to ferrociphenols **2**. This is due to the formation, after their two-electron oxidation, of a new kind of QMs **4**, involving an oxygen-containing heterocycle, in addition to the vinyl QMs **11** (Fig. 4), analogous to those formed upon oxidation of ferrociphenols **2** [42] (Fig. 1 and S2†). To the best of our knowledge, this is the first case involving two such chemotypes of QM pathways from a single substrate, whether in organic or organometallic chemistry. We found that this occurred not only upon oxidation by chemical oxidants such as Ag_2O, but also by enzymatic systems such as HRP in the presence of H_2O_2, or cytochrome P450-dependent monooxygenases that are present in liver microsomes. Evolution of QMs **4** in the incubation medium leads to a surprisingly great diversity of reactive intermediates and final metabolites. After protonation, they lead to rearrangement products such as **5**, **6**, and **10**, and pinacol-type products **9** (Fig. 2). In incubations performed in the presence of an added nucleophile, such as thiols ME, NACM, or

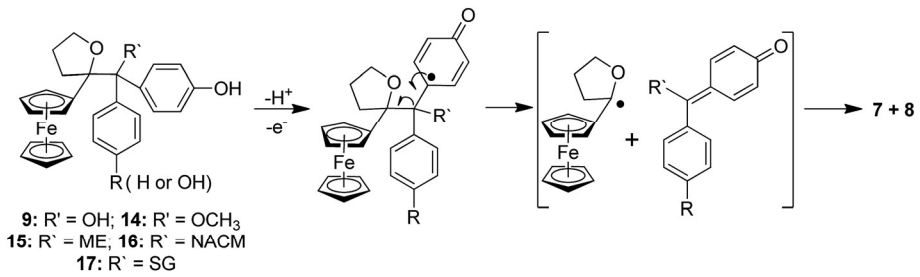

Fig. 6 Possible mechanism for the oxidative cleavage of ferrocenyl pinacol-type compounds by liver microsomes in the presence of NADPH.

GSH, this nucleophile can compete with H_2O for reaction with protonated **4** to give 1,6-thiol adducts **15–17** (Fig. 4). The cleavage of the central C–C bond of intermediates **9**, **14**, **15**, **16**, and **17** further leads to the final stable products **7** and **8**. The mechanism of this C–C bond cleavage remains to be determined. However, one might tentatively propose two possible mechanisms. Firstly, photocleavage of the C–C bond leading to a radical pair has been already proposed (Fig. S1†).[51] Another viable mechanism could be a one-electron oxidation of the phenol function, followed by beta-cleavage of the intermediate radical leading to a radical alpha to the ferrocene ring and a new quinone, the hydrolysis of which would lead to **8**. Further oxidation of the latter radical would lead to **7** (Fig. 6). The particularly high yields of **7** and **8** observed upon oxidation of **3** by liver microsomes in the presence of NADPH would be in favour of the second mechanism, because the radicals formed by one-electron oxidation of the phenol function of compounds **9** and **15–17** by high-valent Fe=O cytochrome P450 species would be generated inside the enzyme active site, and be efficiently oxidized by the Fe^{IV}–OH intermediate to give **7** and **8**.

Comparison of the oxidative metabolism of the hydroxypropyl-ferrociphenols **3** with that of ferrociphenols **2** reveals that a much greater number of reactive, electrophilic intermediates are formed in the former case. This includes the tetrahydrofuran-QMs, **4**, and all the cationic intermediates involved in the formation of **5**, **6** and **9**. Upon protonation, QMs **4** were found to react with a variety of oxygen- and sulfur-containing nucleophiles, such as water, methanol, mercaptoethanol, *N*-acetyl-L-cysteine methyl ester and glutathione, to give the corresponding 1,6-adducts **9**, **14**, **15**, **16**, and **17**. When formed inside the cell, these QMs should covalently react with protein and nucleic acid nucleophiles. The radical intermediates thought to be involved in the formation of 4-hydroxy-1-ferrocenylbutan-1-one, **7**, and the diaryl ketones, **8**, from **9** and **17** could also react with cell macromolecules. Moreover, compounds **5**, **6**, **9**, and **15–17** themselves were also found to have significant antiproliferative properties against breast cancer cells (Table 1).

It is thus likely that the remarkable antiproliferative properties of ferrociphenols **3** are linked to the great diversity of reactive intermediates and metabolites formed during their oxidative metabolism. In that regard, the interesting activity of **3b** towards human ovarian A2780cisR cisplatin resistant cancer cells (Table 2), whose resistance mechanism would refer to an elevated cellular thiol (GSH) level, could be related to a high level of GSH adduct, **17b**, that should exhibit antiproliferative activity. In a more general manner, the great diversity of reactive metabolites formed upon oxidative metabolism of **3** should

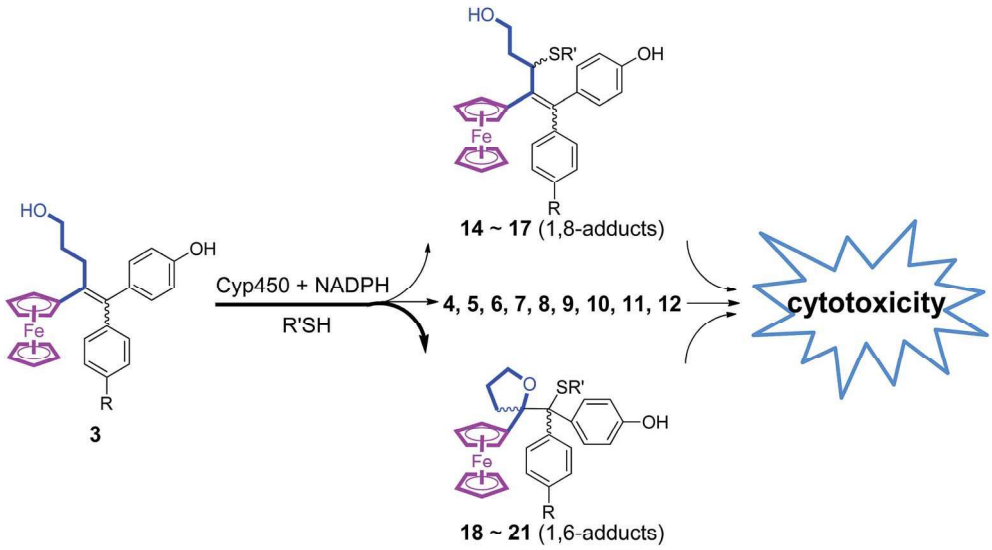

Fig. 7 The diversity of reactive intermediates and metabolites involved in the oxidation of ferrociphenols **3**.

allow them to be more aggressive and cytotoxic for cancer cells that are known to have a higher level of oxidative stress than normal cells. This great diversity of reactive metabolites that could bind to various cell targets should allow them to adapt themselves to various situations existing in cancer cells (Fig. 7). It is well-known that some chemotherapy drugs exert their anticancer effects by forming a diversity of reactive metabolites; typically, 5-fluorouracil is widely used in the treatment of a range of solid tumors, and its mechanism involves the intracellular conversion to several active metabolites.[60,61] The effective cure of acute promyelocytic leukemia by the inorganic drug arsenic trioxide (As_2O_3) is also believed to involve its *in vivo* conversion to yield a diversity of active metabolites.[62]

Further optimization concerning *in vivo* toxicity, mode of administration, pharmacokinetics and pharmacodynamics are currently in progress to maximize the full potential of the hydroxypropyl-ferrociphenols for clinical application. The hydroxypropyl-ferrociphenols **3** not only yield a great diversity of reactive species under metabolic oxidation, but should also be capable of finding the preferential metabolic pathway to accommodate the redox microenvironment of cells. This appears to be the first report of small molecules that are able to achieve a kind of "self-regulation" in terms of the virtual redox microenvironment. This unprecedented metabolic profile may initiate a new strategy for the rational design of anticancer molecules based on prodrugs, thus opening the way to new potent organometallic drug candidates for the treatment of chemoresistant cancers.

Conflicts of interest

There are no conflicts to declare.

Acknowledgements

Y. W. thanks the PGG foundation, PSL University and Feroscan for financial support, and we thank Geoffrey Gontard (IPCM, CNRS UMR 8232) for the X-ray structure determinations, Jérôme Bignon (Plateforme CIBI, ICSN, Gif) for cytotoxicity tests, the National Cancer Institute Developmental Therapeutics Program for *in vitro* testing, Barbara McGlinchey for linguistic assistance and Fatima Mechta-Grigoriou (Insitut Curie, Inserm U830) for helpful disscussions.

References

1 N. S. Gandhi, R. K. Tekade and M. B. Chougule, *J. Controlled Release*, 2014, **194**, 238–256.
2 E. Hutchinson, *Mol. Oncol.*, 2014, **8**, 1–8.
3 F. X. Gu, R. Karnik, A. Z. Wang, F. Alexis, E. Levy-Nissenbaum, S. Hong, R. S. Langer and O. C. Farokhzad, *Nano Today*, 2007, **2**, 14–21.
4 M. O. Palumbo, P. Kavan, W. H. Miller Jr, L. Panasci, S. Assouline, N. Johnson, V. Cohen, F. Patenaude, M. Pollak, R. T. Jagoe and G. Batist, *Front. Pharmacol.*, 2013, **4**, 57.
5 B. Rosenberg and L. Vancamp, *Cancer Res.*, 1970, **30**, 1799–1802.
6 B. Lippert, *Cisplatin: Chemistry and Biochemistry of a Leeding Anticancer Drug*, John Wiley and Sons, New York, 1999.
7 S. Dhar and S. J. Lippard, *Proc. Natl. Acad. Sci. U. S. A.*, 2009, **106**, 22199–22204.
8 P. Zhang and P. J. Sadler, *J. Organomet. Chem.*, 2017, **839**, 5–14.
9 N. P. E. Barry and P. J. Sadler, *Chem. Commun.*, 2013, **49**, 5106–5131.
10 A. A. Nazarov, C. G. Hartinger and P. J. Dyson, *J. Organomet. Chem.*, 2014, **751**, 251–260.
11 G. Gasser, I. Ott and N. Metzler-Nolte, *J. Med. Chem.*, 2011, **54**, 3–25.
12 C. G. Hartinger, N. Metzler-Nolte and P. J. Dyson, *Organometallics*, 2012, **31**, 5677–5685.
13 V. Brabec, S. E. Howson, R. A. Kaner, R. M. Lord, J. Malina, R. M. Phillips, Q. M. A. Abdallah, P. C. McGowan, A. Rodger and P. Scott, *Chem. Sci.*, 2013, **4**, 4407–4416.
14 M. Dörr and E. Meggers, *Curr. Opin. Chem. Biol.*, 2014, **19**, 76–81.
15 L. Oehninger, R. Rubbiani and I. Ott, *Dalton Trans.*, 2013, **42**, 3269–3284.
16 M. A. Cinellu, I. Ott and A. Casini, in *Bioorganometallic Chemistry*, ed. G. Jaouen and M. Salmain, Wiley-VCH, 2015, ch. 4, pp. 117–140.
17 K. D. Mjos and C. Orvig, *Chem. Rev.*, 2014, **114**, 4540–4563.
18 J. J. Soldevila-Barreda, I. Romero-Canelón, A. Habtemariam and P. J. Sadler, *Nat. Commun.*, 2015, **6**, 6582.
19 *Medicinal Organometallic Chemistry*, ed. G. Jaouen and N. Metzler-Nolte, Springerlink, 2010, vol. 32.
20 S. S. Braga and A. M. S. Silva, *Organometallics*, 2013, **32**, 5626–5639.
21 B. Balaji, B. Balakrishman, S. Perumalla, A. A. Karande and A. R. Chakravarty, *Eur. J. Inorg. Chem.*, 2015, **8**, 1398–1407.
22 O. Payen, S. Top, A. Vessieres, E. Brule, M. A. Plamont, M. J. McGlinchey, H. Muller-Bunz and G. Jaouen, *J. Med. Chem.*, 2008, **51**, 1791–1799.
23 K. Kowalski, L. Szczupak, L. Oehninger, I. Ott, P. Hikisz, A. Koceva-Chyla and B. Therrien, *J. Organomet. Chem.*, 2014, **772**, 49–59.
24 J. Amin, I. S. Chuckowree, M. Wang, G. J. Tizzard, S. J. Coles and J. Spencer, *Organometallics*, 2013, **32**, 5818–5825.
25 P. James, J. Neudoerfl, M. Eissmann, P. Jesse, A. Prokop and H.-G. Schmalz, *Org. Lett.*, 2006, **8**, 2763–2766.
26 H. V. Nguyen, A. Sallustrau, J. Balzarini, M. R. Bedford, J. C. Eden, N. Georgousi, N. J. Hodges, J. Kedge, Y. Mehellou, C. Tselepis and J. H. R. Tucker, *J. Med. Chem.*, 2014, **57**, 5817–5822.
27 A. Mooney, R. Tiedt, T. Maghoub, N. O'Donovan, J. Crown, B. White and P. T. M. Kenny, *J. Med. Chem.*, 2012, **55**, 5455–5466.
28 S. B. Deepthi, R. Trivedi, L. Giribabu, P. Sujitha and C. G. Kumar, *Dalton Trans.*, 2013, **42**, 1180–1190.
29 S. Daum, V. F. Chekhun, I. N. Todor, N. Y. Lukianova, Y. V. Shvets, L. Sellner, K. Putzker, J. Lewis, T. Zenz, I. A. M. de Graaf, G. M. M. Groothuis, A. Casini,

O. Zozulia, F. Hampel and A. Mokhir, *J. Med. Chem.*, 2015, **58**, 2015–2024.
30 P. F. Salas, C. Herrmann, J. F. Cawthray, C. Nimphius, A. Kenkel, J. Chen, C. de Kock, P. J. Smith, B. O. Patrick, M. J. Adam and C. Orvig, *J. Med. Chem.*, 2013, **56**, 1596–1613.
31 R. Pulukkody, R. B. Chupik, S. K. Montalvo, S. Khan, N. Bhuvanesh, S.-M. Lim and M. Y. Darensbourg, *Chem. Commun.*, 2017, **53**, 1180–1183.
32 P. Messina, E. Labbe, O. Buriez, E. A. Hillard, A. Vessieres, D. Hamels, S. Top, G. Jaouen, Y. M. Frapart, D. Mansuy and C. Amatore, *Chem.–Eur. J.*, 2012, **18**, 6581–6587.
33 G. Jaouen, A. Vessieres and S. Top, *Chem. Soc. Rev.*, 2015, **44**, 8802–8817.
34 S. Top, J. Tang, A. Vessieres, D. Carrez, C. Provot and G. Jaouen, *Chem. Commun.*, 1996, 955–956.
35 G. Jaouen, S. Top, A. Vessieres, G. Leclercq and M. J. McGlinchey, *Curr. Med. Chem.*, 2004, **11**, 2505–2517.
36 S. Top, A. Vessieres, G. Leclercq, J. Quivy, J. Tang, J. Vaissermann, M. Huche and G. Jaouen, *Chem.–Eur. J.*, 2003, **9**, 5223–5236.
37 G. Jaouen and S. Top, in *Advances in Organometallic Chemistry and Catalysis: The Silver/Gold Jubilee International Conference on Organometallic Chemistry Celebratory Book*, ed. A. J. L. Pombeiro, Wiley, 2014, ch. 42, pp. 563–580.
38 A. Vessieres, C. Corbet, J. M. Heldt, N. Lories, N. Jouy, I. Laios, G. Leclercq, G. Jaouen and R. A. Toillon, *J. Inorg. Biochem.*, 2010, **104**, 503–511.
39 C. Bruyere, V. Mathieu, A. Vessières, P. Pigeon, S. Top, G. Jaouen and R. Kiss, *J. Inorg. Biochem.*, 2014, **141**, 144–151.
40 A. Citta, A. Folda, A. Bindoli, P. Pigeon, S. Top, A. Vessieres, M. Salmain, G. Jaouen and M. P. Rigobello, *J. Med. Chem.*, 2014, **57**, 8849–8859.
41 E. Hillard, A. Vessières, L. Thouin, G. Jaouen and C. Amatore, *Angew. Chem., Int. Ed.*, 2006, **45**, 285–290.
42 Y. Wang, M.-A. Richard, S. Top, P. M. Dansette, P. Pigeon, A. Vessières, D. Mansuy and G. Jaouen, *Angew. Chem., Int. Ed.*, 2016, **55**, 10431–10434.
43 D. Hamels, P. M. Dansette, E. A. Hillard, S. Top, A. Vessieres, P. Herson, G. Jaouen and D. Mansuy, *Angew. Chem., Int. Ed.*, 2009, **48**, 9124–9126.
44 Q. Michard, G. Jaouen, A. Vessieres and B. A. Bernard, *J. Inorg. Biochem.*, 2008, **102**, 1980–1985.
45 E. Allard, C. Passirani, E. Garcion, P. Pigeon, A. Vessières, G. Jaouen and J.-P. Benoit, *J. Controlled Release*, 2008, **130**, 146–153.
46 E. Allard, D. Jarnet, A. Vessieres, S. Vinchon-Petit, G. Jaouen, J. P. Benoit and C. Passirani, *Pharm. Res.*, 2011, **27**, 56–64.
47 A. L. Laine, E. Adriaenssens, A. Vessieres, G. Jaouen, C. Corbet, E. Desruelles, P. Pigeon, R. A. Toillon and C. Passirani, *Biomaterials*, 2013, **34**, 6949–6956.
48 A. L. Laine, A. Clavreul, A. Rousseau, C. Tétaud, A. Vessieres, E. Garcion, G. Jaouen, R. A. Toillon and C. Passirani, *Nanomed. Nanotechnol. Biol. Med.*, 2014, **10**, 1667–1677.
49 Y. Wang, P. Pigeon, S. Top, M. J. McGlinchey and G. Jaouen, *Angew. Chem., Int. Ed.*, 2015, **54**, 10230–10233.
50 R. H. Shoemaker, *Nat. Rev. Cancer*, 2006, **6**, 813–823.
51 I. G. Gut, P. D. Wood and R. W. Redmond, *J. Am. Chem. Soc.*, 1996, **118**, 2366–2373.
52 M.-A. Richard, D. Hamels, P. Pigeon, S. Top, P. M. Dansette, H. Z. S. Lee, A. Vessières, D. Mansuy and G. Jaouen, *ChemMedChem*, 2015, **10**, 981–990.
53 V. Scalcon, A. Citta, A. Folda, A. Bindoli, M. Salmain, I. Ciofini, S. Blanchard, J. D. Cazares-Marinero, Y. Wang, P. Pigeon, G. Jaouen, A. Vessieres and M. P. Rigobello, *J. Inorg. Biochem.*, 2016, **165**, 146–151.
54 D. Wang and S. J. Lippard, *Nat. Rev. Drug Discovery*, 2005, **4**, 307–320.
55 I. Romero-Canelon, L. Salassa and P. J. Sadler, *J. Med. Chem.*, 2013, **56**, 1291–1300.
56 M. Görmen, P. Pigeon, S. Top, E. A. Hillard, M. Huché, C. G. Hartinger, F. de Montigny, M.-A. Plamont, A. Vessières and G. Jaouen, *ChemMedChem*, 2010, **5**, 2039–2050.
57 H. T. Cohen and F. J. McGovern, *N. Engl. J. Med.*, 2005, **353**, 2477–2490.
58 W. T. Bellamy, *Annu. Rev. Pharmacol. Toxicol.*, 1996, **36**, 161–183.
59 D. Grossman and D. C. Altieri, *Cancer Metastasis Rev.*, 2001, **20**, 3–11.
60 D. B. Longley, D. P. Harkin and P. G. Johnston, *Nat. Rev. Cancer*, 2003, **3**, 330–338.
61 P. Álvarez, J. A. Marchal, H. Boulaiz, E. Carrillo, C. Vélez, F. Rodríguez-Serrano, C. Melguizo, J. Prados, R. Madeddu and A. Aranega, *Expert Opin. Ther. Pat.*, 2012, **22**, 107–123.
62 G.-Q. Chen, L. Zhou, M. Styblo, F. Walton, Y. Jing, R. Weinberg, Z. Chen and S. Waxman, *Cancer Res.*, 2003, **63**, 1853–1859.